imaginary frequencies. This shows that it is a two-dimensional saddle point (a transition state between transition states).

We compare finally the computed transition states with the literature proposals (see Figure 1). Neither the proposal of Gerig and Roberts[6] (G) nor that of De Pessemier, Anteunis, and Tavernier[7] (D) corresponds to the lowest transition state calculated here. Proposal G resembles best the high-energy transition states ts4-6. The geometry of proposal D is not too well reproduced in any of the computed transition states, but it is between ts7 and ts8, with the former one being the better approximation. Thus, the main idea of proposal D, a transition state with a small torsion angle around the central bond, is borne out by the computed transition states of lowest energy.

Acknowledgment. Professor Anteunis is thanked for his interest in this work.

Mechanism and Kinetic Characteristics of the Electrochemical Reduction of Carbon Dioxide in Media of Low Proton Availability

Christian Amatore and Jean-Michel Savéant*

Contribution from the Laboratoire d'Electrochimie de l'Université Paris 7, 75251 Paris Cedex 05, France. *Received January 28, 1981*

Abstract: The mechanism of the reduction of carbon dioxide in solvents of low proton availability such as dimethylformamide is investigated on the basis of the variation of the electrolysis product distribution with current density and concentration of CO_2 and water. It is shown to involve three competing pathways: oxalate formation through self-coupling of the $CO_2^{-}\cdot$ anion radicals, CO formation via oxygen–carbon coupling of $CO_2^{-}\cdot$ with CO_2, and formate formation through protonation of $CO_2^{-}\cdot$ by residual or added water followed by an homogeneous electron transfer from $CO_2^{-}\cdot$. Using the product distribution data together with the kinetic data obtained by fast microelectrolytic techniques allows the characterization of the key steps of the reduction process: initial electron transfer and the rate determining steps of the three competing reactions leading to oxalate, CO, and formate.

Carbon dioxide is an abundant and low-cost potential source of carbon for the production of fuels and organic chemicals. Electrochemical reduction provides a means of activating this particularly inert molecule. The nature of the reduction products crucially depends upon the reaction medium. In water, formic acid is the main product[1-4]

$$2CO_2 + H_2O + 2e^- \rightarrow HCO_2^- + HCO_3^-$$

while oxalate and carbon monoxide are obtained together with formate in solvents of low proton availability such as dimethylformamide, dimethyl sulfoxide, and propylene carbonate (see ref 3 and 5 and references cited therein).

$$2CO_2 + 2e^- \rightarrow C_2O_4^{2-}$$

$$2CO_2 + 2e^- \rightarrow CO + CO_3^{2-}$$

The addition of small amounts of water not only favors the formation of formate but also induces further reduction of oxalate, mainly into glycolate.[3,5]

Application of electrochemical[6] and spectroelectrochemical[7] microelectrolytic techniques, although providing some interesting thermodynamic and kinetic data, has not been able to give a description of the reaction mechanism and of the factors that determine the relative importance of the competing pathways leading to the various products. As made clear in the following, the distribution of products strongly depends upon operational factors such as current density, concentration, and diffusion layer thickness. This renders uncertain the extrapolation of results obtained in the context of microelectrolytic techniques to the conditions prevailing in macroscale electrolysis.

The discussion of the reaction mechanism and of the competition factors should thus mainly rely upon the determination of the distribution of products in preparative scale electrolysis and its systematic variations with the electrolysis parameters. This question has been addressed recently[5] leading to the proposal of the reaction mechanism depicted in Scheme I. However this scheme was developed on a qualitative basis, allowing no kinetic

Scheme I

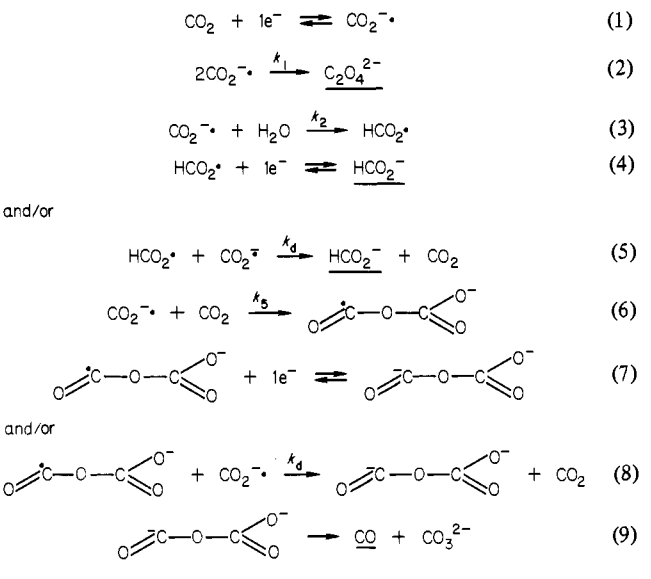

(1) Roberts, J. L.; Sawyer, D. T. *J. Electroanal. Chem.* **1965**, *9*, 1.
(2) Paik, N.; Andersen, T.; Eyring, H. *Electrochim. Acta* **1969**, *16*, 1217.
(3) Kaiser, V.; Heitz, E. *Ber. Bunsen. Gesell.*, **1973**, *77*, 818.
(4) Russel, P. G.; Novac, N.; Srinivasan, S.; Steinberg, M. *J. Electrochem. Soc.* **1977**, *124*, 1329.
(5) Gressin, J. C.; Michelet, D.; Nadjo, L.; Savéant, J.-M. *Nouv. J. Chim.* **1979**, *3*, 545.
(6) Lamy, E.; Nadjo, L.; Savéant, J.-M. *J. Electroanal. Chem.* **1977**, *78*, 403.
(7) Aylmer-Kelly, A. W. B.; Bewick, A.; Cantrill, P. R.; Tuxford, A. M. *Discuss. Faraday Soc.* **1973**, *56*, 96.

0002-7863/81/1503-5021$01.25/0

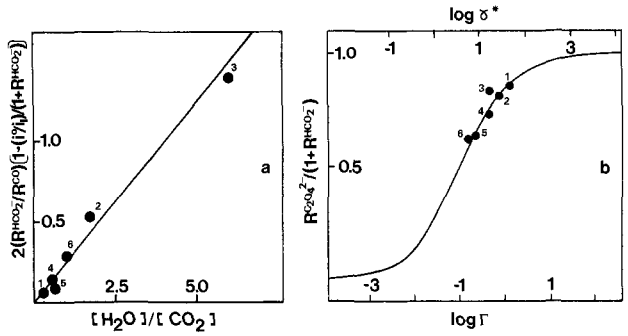

Number of the experiment	1	2	3	4	5	6
i^0/i_1	0.27	0.28	0.32	0.12	0.06	0.12
$[CO_2]$ (M)	0.166	0.130	0.039	0.124	0.124	0.130
(H_2O) (M)	0.045	0.233	0.236	0.080	0.090	0.156
$R^{C_2O_4^{2-}}$	0.86	0.85	0.88	0.74	0.64	0.65
R^{CO}	0.13	0.11	0.06	0.24	0.35	0.30
$R^{HCO_2^-}$	0.006	0.04	0.05	0.02	0.01	0.05
$10^3\delta$ (cm)	1.4	1.4	3.0	1.4	1.4	3.0

Figure 1. Electrochemical reduction CO_2 on mercury in DMF: (a) correlation between the formate and CO yields; (b) correlations between the oxalate, formate, and CO yields (for the definition of γ^* and Γ, see text).

characterization owing to the lack of a theory relating the product distribution to the intrinsic (rates, diffusion coefficients) and operational (concentrations, current density, thickness of the diffusion layer) parameters of the system. Such a theory was recently made available,[8] allowing a sounder demonstration of the reaction mechanism and the determination of the characteristic rate constants. This was the aim of the work reported hereafter on the basis of product distribution data previously determined for electrolyses carried out in DMF on mercury and lead electrodes.

Results and Discussion

Starting with the above reaction scheme, it is predicted that the yields of formate, $R^{HCO_2^-}$ and of carbon monoxide, R^{CO}, should be interrelated through eq 10[8]for electrolyses carried out at

$$2(R^{HCO_2^-}/R^{CO})[1 - (i^0/i_1)/(1 + R^{HCO_2^-})] = (k_2/k_5)([H_2O]/[CO_2]) \quad (10)$$

constant current, the concentration of the substrate being held constant throughout electrolysis, where i^0 ($i^0 < i_1$) is the imposed current intensity and i_1 is the current intensity at the plateau of the wave, $i_1 = FSD[CO_2]/\delta$ (S is electrode surface area, δ is diffusion layer thickness, and D is diffusion coefficient of CO_2). As shown in Figure 1a, the predicted linear relationship is satisfactorily followed (the correlation coefficient is 0.98)[9] by the data obtained for the reduction of CO_2 on a mercury electrode in DMF at various current densities and concentrations of CO_2 and water.[5] From this, the rate constant ratio k_2/k_5 is found equal to 0.24.

Regarding the yields of oxalate, $R^{C_2O_4^{2-}}$, of formate, and of CO, another interesting correlation is predicted to hold on the basis

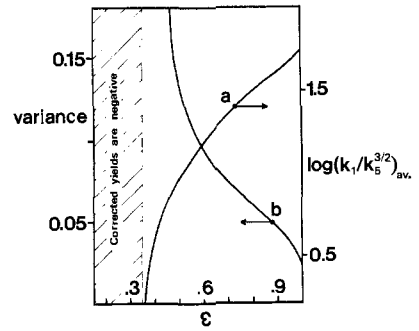

Figure 2. Average value of log ($k_1k_5^{-3/2}$) and variance as a function of ϵ (see text): (a) average value; (b) variance.

of the same reaction scheme: the ratio $R^{C_2O_4^{2-}}/(1 + R^{HCO_2^-})$ should vary with the parameter

$$\gamma^* = k_1k_5^{-3/2}(D/2[CO_2])^{1/2}\delta^{-1}(i^0/i_1)\{(1 + 2R^{HCO_2^-}/R^{CO}) \times [1 - (i^0/i^1)/(1 + R^{HCO_2^-})]\}^{-3/2}$$

as represented on figure 1b (full line).[8] It is found that the results obtained on mercury in DMF[5] are again in good agreement with the predicted behavior[10] under the form of a $R^{C_2O_4^{2-}}/(1 + R^{HCO_2^-})$ vs. log Γ plot (Figure 1b). Γ is defined as $\Gamma = \gamma^*k_1^{-1}k_5^{3/2}$ and thus only contains, as seen from the above equation, measurable quantities. Fitting of the theoretical working curve with the experimental points thus leads to the rate factor $k_1k_5^{-3/2}$, which was then found to be 56 $M^{1/2}$ $s^{1/2}$.

A first conclusion is thus that the proposed mechanism correctly fits the experimental data obtained at a mercury electrode. Another mode for the formation of oxalate has however previously been postulated:[7] it would involve a carbon–carbon coupling of $CO_2^{-}\cdot$ with CO_2 instead of a radical–radical dimerization of $CO_2^{-}\cdot$. Although not in agreement with previous ESR data[13] and with the observation that the anion radical resulting from the one-electron oxidation of oxalate in acetonitrile cleaves rapidly,[14] it is interesting to see if the preparative scale data can also rule out this mechanistic possibility. We thus now consider that oxalate can be formed along two competing routes: reactions 2 and 11

$$CO_2^{-}\cdot + CO_2 \longrightarrow \text{(oxalate radical)} \quad (11)$$

$$\text{(oxalate radical)} + 1e^- \rightleftharpoons C_2O_4^{2-} \quad (12)$$

$$\text{(oxalate radical)} + CO_2^{-}\cdot \longrightarrow C_2O_4^{2-} + CO_2 \quad (13)$$

followed by reaction 12 and/or 13. This pathway for forming oxalate thus strictly parallels that leading to carbon monoxide through carbon–oxygen coupling (eq 6). Let ϵ be the fraction of $CO_2^{-}\cdot$ disappearing through reaction 6 and $1 - \epsilon$ the fraction undergoing reaction 11. When $R^{C_2O_4^{2-}}$ is replaced by $R^E = R^{C_2O_4^{2-}} - [(1 - \epsilon)/\epsilon]R^{CO}$ and R^{CO} by $R^F = R^{CO}/\epsilon$ with $R^{HCO_2^-}$ remaining

(8) Amatore, C.; Savéant, J.-M. *J. Electroanal. Chem.*, in press.
(9) The theoretical analysis assumed that reaction 3 is pseudo first order. Several points on Figure 1a correspond to a $[H_2O]/[CO_2]$ ratio less than unity and nevertheless fit the predicted behavior. This stems from the fact that they correspond to a very small formation of formate and thus a very small consumption of water, as compared to the initial water concentration.

(10) The whole analysis was carried out under the assumption that the heterogeneous electron-transfer reactions (4) and (7) interfere negligibly as compared to the corresponding homogeneous electron-transfer steps (5) and (8). This is in fact consistent with the values found for k_2/k_5 and $k_1k_5^{-3/2}$ the self-coupling rate constant k_1 is at maximum equal to the diffusion limit (10^{10} M^{-1} s^{-1} in DMF[11]) and thus $k_5 < 3 \times 10^5$ $M^{-1}s^{-1}$ and the pseudo-first-order rate constant for reaction 6[8] $k_5[CO_2][1 - (i^0/i_1)/(1 + R^{HCO_2^-}] < 3 \times 10^4$ s^{-1}; on the other hand, $k_2 < 10^4$ s^{-1} and thus the two first-order rate constant are small enough for the heterogeneous electron transfers to be neglected as opposed to the homogeneous electron transfers. These conclusions based on a quantitative analysis of the "Ece-Disp" (heterogeneous vs. homogeneous electron transfers) problem[12] derive qualitatively from the following picture k_2 and k_5 being relatively small, $HCO_2\cdot$ and $O{=}C{-}O{-}CO_2^-$ are formed far from the electrode surface. They will thus be reduced by $CO_2^{-}\cdot$ in the solution before having time to diffuse back to the electrode surface and be reduced there.

(11) Andrieux, C. P.; Blocman, C.; Dumas-Bouchiat, J. M.; M'Halla, F.; Savéant, J.-M. *J. Am. Chem. Soc.* **1980**, *102*, 3806.
(12) Amatore, C.; Savéant, J.-M. *J. Electroanal. Chem.* **1981**, *123*, 189.
(13) Overral, D. W.; Whiffen, D. H. *Mol. Phys.* **1961**, *4*, 113.
(14) Cahng, M. M.; Saji, T.; Bard, A. J. *J. Am. Chem. Soc.* **1977**, *99*, 5399.

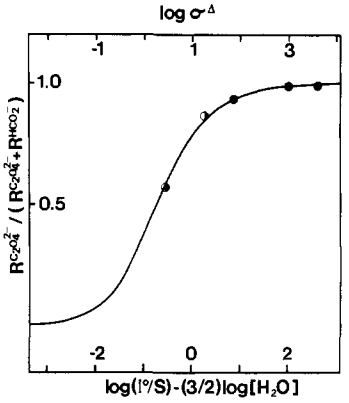

Figure 3. Electrochemical reduction of CO_2 on lead in DMF at high current densities. Variations of $R^{C_2O_4^{2-}}/(R^{C_2O_4^{2-}} + R^{HCO_2^-})$ with current density and water concentration (◑: data corrected from the amount of glycolate formed).

the same and k_2/k_5 being substituted by $k_2/\epsilon k_5$, the preceding kinetic analysis remains formally the same. The treatment of the experimental data along these lines for various values of ϵ shows (Figure 2) that the best fit is obtained for $\epsilon = 1$. The variance for the statistical treatment of the experimental data had indeed its minimal value at $\epsilon = 1$ (curve b on figure 2). This points to the conclusion that carbon–oxygen coupling of $CO_2^{-}\cdot$ with CO_2 appears as a negligible pathway for the formation of oxalate.

Since k_2/k_5 and $k_1/k_5^{3/2}$ are now known, knowledge of one of these rate constants would allow the determination of all three. An estimate of $k_1 \simeq 10^7$ M^{-1} s^{-1} can be derived from previous cyclic voltammetric experiments in DMF in the kilovolt per second sweep rate range.[6] It is indeed possible to show that under these experimental conditions step 2 kinetically predominates over steps 3 and 6.[15] This leads to the following characterization of the essential reaction steps for the reduction of CO_2 in DMF at a mercury electrode: initial electron transfer, standard potential, $E° = -2.21$ V vs. SCE; transfer coefficient, $\alpha = 0.4$; standard rate constant, $k^{ap} = 6 \times 10^{-3}$ cm s^{-1}; carbon–carbon self coupling of the CO_2 anion radical, $k_1 = 10^7$ M^{-1} s^{-1}; oxygen–carbon coupling of $CO_2^{-}\cdot$ with CO_2, $k_5 = 3.2$ 10^3 M^{-1} s^{-1}; neutralization of $CO_2^{-}\cdot$ by water leading to formate, $k_2 = 7.7 \times 10^2$ M^{-1} s^{-1}.

Data for the reduction of CO_2 in DMF on a lead electrode[5] have been obtained at significantly higher current densities than on mercury for comparable CO_2 concentrations and stirring rates. This explains why the yields in oxalate were found to be higher than on mercury without the need of invoking a specific interaction of $CO_2^{-}\cdot$ with the lead surface.[5] The formation of CO can practically be neglected for a large part of the data obtained on lead.[5] These data can thus be treated according to a scheme which accordingly neglect reaction 6. It is then predicted that the yield of oxalate will vary with the parameter[16]

$$\sigma^{\Delta} = k_1 k_2^{-3/2} D^{-1/2}[H_2O]^{-3/2} \quad (i^0/FS)$$

along the working curve shown on Figure 3. The agreement between experimental data and predicted behavior is seen to be satisfactory. Fitting of the theoretical working curve with the experimental points leads to $k_1 k_2^{-3/2} = 306$ $M^{1/2}$ $s^{1/2}$. This is to be compared with the value of $k_1 k_2^{-3/2} = 475$ $M^{1/2}$ $s^{1/2}$ found on mercury. It is noted in this respect that the geometrical apparent electrode surface area was used in the treatment of the results obtained on lead. Unevenness of the electrode surface may, however, well be such that the actual surface area is on the order of one and a half times the geometrical apparent value which would reconcile the results obtained on lead and on mercury. We may therefore conclude that the apparent difference in kinetic constants between lead and mercury is not such as to indicate a specific chemical effect of the metal on the course of CO_2 reduction.

In view of these conclusions it is interesting to reexamine the results obtained in the investigation of the CO_2 reduction in propylene carbonate on a lead electrode by means of modulated specular reflectance spectroscopy.[7] Taking for the rate constants k_1 and k_5 values on the same order of magnitude as those found in DMF and assuming the formation of about the same amount of oxalate and CO, it is possible to simulate satisfactorily the kinetic data given under the form of a plot of the current density vs. the total amount of $CO_2^{-}\cdot$ taking into account uncertainties pertaining to the value of the extinction coefficient and the magnitude of the residual current. These spectroelectrochemical results are thus in general agreement with our conclusions on the basis of the analysis of product distribution in preparative scale electrolysis.

In summary, the reduction of CO_2 in media of low proton availability appears to involve three competitive pathways: oxalate formation through self-coupling of $CO_2^{-}\cdot$, CO formation *via* oxygen–carbon coupling of $CO_2^{-}\cdot$ with CO_2, and formate formation through protonation of $CO_2^{-}\cdot$ by residual or added water followed by an electron transfer occurring in the solution, the electron source being $CO_2^{-}\cdot$ itself. Using the kinetic data obtained by means of fast microelectrolytic techniques together with those of a systematic investigation of the product distribution allows a rather complete characterization of the key steps of the reduction process, i.e., the initial electron-transfer reaction and the rate-determining steps of the three competing processes leading to oxalate, CO, and formate. The less precise determination concerns the self-coupling rate constant k_1, which consequently affects the values of k_2 and k_5, whereas the rate factors k_2/k_5 and $k_1/k_5^{3/2}$ are determined with more accuracy.

Acknowledgment. Support by the CNRS (ATP "Energie et Matières Premières" 1979; Electrochimie Sélective) is acknowledged.

(15) Since the experiments were carried out in the presence of activated alumina, reaction of $CO_2^{-}\cdot$ on residual water (eq 3) can be neglected. An approximate treatment of the competition between reactions 1 and 5 in the context of cyclic voltammetry leads to the introduction of the competition parameters $\gamma^{LSV} = k_1 k_5^{-3/2} \Psi_p(1 - \Psi_p)^{-3/2}(2C°)^{-1/2}(Fv/RT)^{1/2}$ (Ψ_p is the dimensionless form of the peak current, i_p; $\psi_p = i_p/FS[CO_2]D^{1/2}(Fv/RT)^{1/2}$, v is the sweep rate). In the conditions of the experiments γ is on the order of 10^5, i.e., largely in favor of self-coupling with CO_2.

(16) Amatore, C.; Savéant, J.-M. *J. Electroanal. Chem.*, in press.